Development 134, 1011-1022 (2007) doi:10.1242/dev.02789

Sdf1a patterns zebrafish melanophores and links the somite and melanophore pattern defects in *choker* mutants

Valentina Svetic[1,*], Georgina E. Hollway[2,*], Stone Elworthy[3], Thomas R. Chipperfield[1], Claire Davison[3], Richard J. Adams[1,4], Judith S. Eisen[5], Philip W. Ingham[3], Peter D. Currie[2] and Robert N. Kelsh[1,†]

Pigment pattern formation in zebrafish presents a tractable model system for studying the morphogenesis of neural crest derivatives. Embryos mutant for *choker* manifest a unique pigment pattern phenotype that combines a loss of lateral stripe melanophores with an ectopic melanophore 'collar' at the head-trunk border. We find that defects in neural crest migration are largely restricted to the lateral migration pathway, affecting both xanthophores (lost) and melanophores (gained) in *choker* mutants. Double mutant and timelapse analyses demonstrate that these defects are likely to be driven independently, the collar being formed by invasion of melanophores from the dorsal and ventral stripes. Using tissue transplantation, we show that melanophore patterning depends upon the underlying somitic cells, the myotomal derivatives of which – both slow- and fast-twitch muscle fibres – are themselves significantly disorganised in the region of the ectopic collar. In addition, we uncover an aberrant pattern of expression of the gene encoding the chemokine Sdf1a in *choker* mutant homozygotes that correlates with each aspect of the melanophore pattern defect. Using morpholino knock-down and ectopic expression experiments, we provide evidence to suggest that Sdf1a drives melanophore invasion in the *choker* mutant collar and normally plays an essential role in patterning the lateral stripe. We thus identify Sdf1 as a key molecule in pigment pattern formation, adding to the growing inventory of its roles in embryonic development.

KEY WORDS: Neural crest, Migration, Patterning, Pigment pattern formation, Melanophore, Melanocyte, Xanthophore, Chromatophore, Slow muscle, Fast muscle, Horizontal myoseptum, *cho*, *you*-type, Sdf1a (Cxcl12a), Zebrafish

INTRODUCTION

The neural crest (NC) is a transient tissue that generates many important structures, including much of the peripheral nervous system, cranial skeleton and body pigmentation. Correct patterning of NC derivatives is achieved through regulation of cell migration and involves both environmental and cell-autonomous factors (Perris and Perissinotto, 2000; Krull, 2001). The somites have particular importance in patterning NC migration, as is perhaps best characterised in developing chick dorsal root ganglia (Lallier and Bronner-Fraser, 1988). Here, NC migrates on a ventral pathway (between somites and neural tube; called the medial pathway in zebrafish) only through the rostral portion of each sclerotome (Rickmann et al., 1985). This patterned migration results from differential expression of migration-promoting molecules such as thrombospondin, and migration-inhibiting molecules such as F-spondin and ephrin ligands, in rostral and caudal sclerotome, respectively (Davies et al., 1990).

Mechanisms regulating migration on the dorsolateral (lateral pathway in zebrafish) pathway, between the skin and dermomyotome, are incompletely understood. Timelapse studies in zebrafish reveal that premigratory NC cells extend numerous protrusions that actively explore the lateral migration pathway. Before lateral pathway migration begins, these protrusions undergo rapid collapse, apparently because of somite-associated inhibitory activity (Jesuthasan, 1996). Later, the frequency of protrusion collapse decreases, allowing migration over the somite. Similarly, lateral pathway 'maturation' is indicated by heterologous extracellular matrix (ECM) transplantation studies in axolotl, with precocious NC migration initiated by ECM from older embryos (Löfberg et al., 1985; Löfberg et al., 1989). Two signals controlling the time when migration begins have been identified. Kit ligand attracts melanoblasts onto the dorsolateral pathway in mouse (Wehrle-Haller and Weston, 1995) and, in chick, ephrinB acting via EphB receptors regulates which neural crest cell types migrate on the dorsolateral pathway (Santiago and Erickson, 2002). In mouse and chick, only melanocytes utilise the dorsolateral pathway, and these become distributed ubiquitously, whereas in fish, several distinct types of chromatophores use this pathway and pigment pattern formation results from controlling their migration and final positioning (Kelsh, 2004).

In zebrafish embryos, pigment patterns form from three chromatophore types. Black melanophores (equivalent to mammalian melanocytes) are principally arranged in four longitudinal stripes, including dorsal and ventral stripes extending from the head to the tip of the tail and the lateral stripe along the horizontal myoseptum of somites 6-26 (Kelsh et al., 1996). Iridescent iridophores are found within some melanophore stripes, whereas yellow xanthophores lie scattered throughout the embryo flank. The prominence and reproducibility of their pigment patterns make zebrafish ideally suited for mutant screens to identify NC patterning cues. Numerous loci necessary for correct development of embryonic (Kelsh et al., 1996; Odenthal et al., 1996) and adult (Haffter et al., 1996; Parichy et al., 2000a) zebrafish pigment cells have been identified. As with the pigment mutant collections in mice (Lyon and Searle, 1989), zebrafish pigmentation mutants exhibit a changed

[1]Centre for Regenerative Medicine and Developmental Biology Programme, Department of Biology and Biochemistry, University of Bath, Bath BA2 7AY, UK. [2]Victor Chang, Cardiac Research Institute, 384 Victoria Street, Darlinghurst, Sydney 2010, Australia. [3]MRC Centre for Developmental and Biomedical Genetics, University of Sheffield, Firth Court, Western Bank, Sheffield S10 2TN, UK. [4]Department of Anatomy, University of Cambridge, Downing Street, Cambridge CB2 3DY, UK. [5]Institute of Neuroscience, University of Oregon, Eugene, OR 97403, USA.

*These authors contributed equally to this work
[†]Author for correspondence (e-mail: bssrnk@bath.ac.uk)

Accepted 18 December 2006

appearance to the body pigmentation and are commonly referred to as 'pigment pattern mutants', although only a small subclass of the pigment pattern mutants actually has altered pigment cell positions. Studies of fish pigment pattern mutants (*sensu stricto*) have focused to date on the adult pattern (Asai et al., 1999; Johnson et al., 1995; Rawls and Johnson, 2001; Parichy and Turner, 2003; Quigley et al., 2004), but this is likely to be under very different control from the embryonic pigment pattern.

Stromal cell-derived factor 1 (SDF1; CXCL12 – Human Gene Nomenclature Database) in humans is the ligand for CXCR4, a G-protein-coupled receptor known for its role in both leukocyte and neural stem cell migration and as a co-receptor for HIV-1 (Feng et al., 1996; Imitola et al., 2004; Loetscher et al., 1994; Oberlin et al., 1996). Zebrafish have two SDF1 and two CXCR4 orthologues (Chong et al., 2001; David et al., 2002; Doitsidou et al., 2002; Knaut et al., 2003; Li et al., 2004; Li et al., 2005). Zebrafish mutant and morphant studies demonstrate that Cxcr4b-Sdf1a (Cxcl12a – Zebrafish Information Network) signalling is necessary for correct migration of primordial germ cells, the posterior lateral line (PLL) primordium, retinal ganglion cell axons and hindbrain neuron cell bodies (David et al., 2002; Doitsidou et al., 2002; Gilmour et al., 2004; Knaut et al., 2003; Li et al., 2004). Further study in zebrafish germ cells has dissected specific roles for distinct intracellular signalling pathways in driving the motility and directionality of response to Sdf1a signalling (Dumstrei et al., 2004). *cxcr4b* is expressed in the migrating cells, whereas *sdf1a* expression neatly delineates the migration routes. The PLL primordium migration route coincides with the position of the lateral stripe melanophores; whether or not Sdf1a activity contributes to their patterning is currently unknown.

The *choker* (*cho*) mutant was identified in the Tübingen 1996 genetic screen and was classified as a '*you*-type' (*you* is also known as *scube2* – Zebrafish Information Network) muscle mutant, so named because of the U-shaped appearance of their somites [V-shaped in wild type (WT)], a phenotype thought to be due to a lack of structural integrity resulting from loss of the horizontal myoseptum (van Eeden et al., 1996). Zebrafish myotomes consist of two types of slow-twitch muscle fibres and fast-twitch muscle fibres. Most somite cells develop into fast-twitch muscles, whereas slow muscle fibres derive from adaxial cells developing adjacent to the notochord. Most adaxial cells migrate laterally to form a subcutaneous layer of surface slow muscle fibres by 24 hours post-fertilisation (hpf) (Devoto et al., 1996), whilst a few develop into muscle pioneer fibres located at the position of the future horizontal myoseptum. Hedgehog signalling is necessary for specification of slow muscle cells (Currie and Ingham, 1996; Blagden et al., 1997), and most *you*-type mutants affect the production or transduction of the Hedgehog signals (Schauerte et al., 1998; Karlstrom et al., 1999; Barresi et al., 2000; Kawakami et al., 2005; Nakano et al., 2004; Woods and Talbot, 2005). PLL primordium migration is aberrant in *you*-type mutants owing to the loss of *sdf1a* expression from the horizontal myoseptal region (David et al., 2002; Li et al., 2004). In addition, they all show a pigment pattern defect: lateral stripe melanophores are completely absent (Kelsh et al., 1996). Uniquely, *cho* mutants also have an ectopic melanophore band (collar) spanning the anterior-most five somites and bridging the dorsal and ventral stripes. Despite the absence of the lateral stripe, and in contrast to the other *you*-type mutants, muscle pioneer cells differentiate normally in *choker* mutant embryos. We find, however, that both slow- and fast-twitch muscle fibres are patterned aberrantly in the anterior-most somites and there is a general disorganisation of myotomal architecture in this region. We show by somite transplantation experiments that the pigment defects occur as secondary consequences of abnormal somite development.

We have investigated the timing of melanophore accumulation and the mechanism of ectopic collar formation. Collar formation corresponds to a post-migratory phase for NC cells in WT and defects are restricted to two pigment cell types, both of which utilise the lateral migratory pathway. Our results suggest that the two defects are independent and show that the ectopic collar forms by aberrant invasion of melanophores from both dorsal and ventral stripes. Observing abnormal *sdf1a* expression in *cho* mutant somites, we uncover a role for Sdf1a in melanophore patterning in both lateral stripe generation in WT and melanophore collar formation in *cho* mutants.

MATERIALS AND METHODS

Fish husbandry

Embryos were obtained by natural crosses, staged according to Kimmel et al. (Kimmel et al., 1995) and reared in Embryo Medium (Kimmel and Warga, 1987) at 28.5°C. The following mutant alleles were used: cho^{tm26} (Kelsh et al., 1996; van Eeden et al., 1996) and $nacre^{w2}$ (Lister et al., 1999). Double mutants were created by crossing identified carriers for the single mutant alleles; offspring were reared to adulthood and carriers for both alleles were identified in the expected mendelian ratios.

Whole-mount RNA in situ hybridisation, immunocytochemistry and Alcian Blue staining

RNA in situ hybridisation was performed according to Kelsh et al. (Kelsh et al., 2000b). Probes used were as follows: *dopachrome tautomerase* (*dct*) (Kelsh et al., 2000b), *nacre* (*mitfa*) (Lister et al., 1999), *GTP cyclohydrolase 1* (*gch*) (Parichy et al., 2000b), *sdf1a* (David et al., 2002), *engrailed* (Ekker et al., 1992) and *smbp* (Neyt et al., 2000). To partially inhibit melanisation, embryos were placed in 0.003% phenyl-thio-urea (PTU) in Embryo Medium and reared normally.

Antibody staining was performed using anti-Hu mAb 16A11 (Marusich et al., 1994) and anti-acetylated tubulin (Sigma) primary antibodies and detected with Alexa fluor secondary antibodies (Molecular Probes). The anti-Engrailed mAb 4D9 was detected with DAB (Vector Laboratories). F59 (Crow and Stockdale, 1986) antibody staining was performed using peroxidase-antiperoxidase (Sternberger Monoclonals). Antibody staining with fast muscle-specific EB165 and slow muscle-specific BAD5 was performed as described in Lewis et al. (Lewis et al., 1999). Pan-myosin antibody MF20 was detected using a TcsSP confocal microscope (Leica).

Alcian Blue staining of craniofacial cartilage was performed according to Kelsh and Eisen (Kelsh and Eisen, 2000).

For microscopy, live embryos were anaesthetised with 0.003% tricaine (Sigma), examined under an Eclipse E800 compound microscope (Nikon) and photographed with a U-III (Nikon) or a Spot (Diagnostic Instruments) camera.

Melanophore counts

Embryos were reared to the required developmental stages, then anaesthetised in 0.003% tricaine in Embryo Medium and fixed in 4% paraformaldehyde. Melanophores were counted on the lateral pathway over the first five somites on both sides of each embryo on an Eclipse E800 microscope; cells with 25% or more of their area on the lateral pathway were included. Melanophore counts in *sdf1a* morphant studies were counted after fixation in 4% paraformaldehyde on an Olympus IX70 inverted microscope.

Timelapse microscopy

Embryos were dechorionated and anaesthetised in 0.003% tricaine in Embryo Medium and immobilised in 0.5% agarose 0.003% tricaine in Embryo Medium on a circular glass coverslip, which was placed into a metal chamber. The chamber was filled with Embryo Medium and a small amount of perfluorodecalin (F2 Chemicals) that had been saturated with oxygen by bubbling prior to addition to the chamber. The chamber was sealed with another glass coverslip and observed under an Eclipse E1000 (Nikon)

microscope, using a 20× dry objective. The microscope stage was surrounded by a heated chamber maintained at approximately 30°C. Images were collected for up to 30 hours with a Hamamatsu C4880 CCD camera, and processed using Metamorph software (Universal Imaging, USA). Development appeared normal, although somewhat slowed. Timelapses were started at either 30 or 48 hpf, with WT and *cho* mutant embryos mounted together and observed in parallel.

Confocal microscopy

Embryos were collected at 24 hpf, dechorionated, and stained with F59 antibody as described by Lewis et al. (Lewis et al., 1999) except that the antibody was detected fluorescently. Labelled embryos were mounted in glycerol under a coverslip and imaged with the Zeiss LSM510 confocal system. Confocal sections were rendered and animated using the LSM510 system software.

Somite transplantation and bead implantation

Somite transplantation was performed as previously described (Haines et al., 2004). Bead implantation utilised a novel method of agarose adhesion to avoid puncture of the epidermis. AffiGel Blue Gel beads (Biorad) were rinsed several times, soaked in a 1 μg/μl solution of recombinant human SDF1 (Chemicon International, CA) in water, and then rinsed and stored in water until use, usually within 5 hours. Control beads were rinsed in water before agarose mounting. Embryos were embedded in 0.7% agarose on coverslips. Agarose was dissected away and an SDF1-soaked bead was placed next to the skin. More agarose was added to hold the bead in place and, where possible, agarose was dissected away from the head, heart region and tail. Embryos were incubated at 28.5°C for the desired period.

Morpholino injection

Morpholino oligonucleotide *sdf1a*-Mo (5′-ATCACTTTGAGATC**CAT**-GTTTGCA-3′; translation start site is indicated in bold) was obtained from GeneTools (Philomath, OR) and was injected at 1.0 mM. This morpholino is of identical sequence to that used previously (David et al., 2002), and our injected embryos had consistent misrouting of the PLL nerve as described by these authors.

RESULTS

cho mutants accumulate ectopic melanophores in late embryonic development as a result of persistent lateral pathway migration

We characterised the timing of collar formation by counting melanophores on the lateral pathway in the anterior trunk of *cho* mutants and WT at intervals between 30 and 60 hpf (Fig. 1). At 30 hpf, both *cho* mutants and WT had comparable numbers, but by 36 hpf *cho* mutants showed a slight increase in melanophores in this region. Over the next 12 hours, the number of melanophores in the WT decreased, becoming minimal by 54 hpf. By contrast, melanophores continued to accumulate in the collar region of *cho* mutants. By 48 hpf, *cho* mutants had a rudimentary collar, which continued to accumulate melanophores.

Timelapse microscopy revealed melanophore behaviour during collar formation. We studied *cho* mutant and WT embryos from 24 hpf, when collar formation was initially not obvious, and from 48 hpf, when *cho* mutants were readily sorted by their melanophore collars. Timelapses of 24 hpf embryos for over 15 hours showed indistinguishable melanophore behaviour in this early phase. Both WT and *cho* mutant melanophores were highly motile, frequently migrating on the lateral pathway in both dorsoventral and ventrodorsal directions; frequent changes of direction and temporary cessation of migration induced by contact with another melanophore were also observed (data not shown). Towards the end of these early timelapses, melanophores in the WT evacuated the collar region, whilst in *cho* mutants one or two melanophores remained in the collar region. That this behaviour represented the beginning of collar

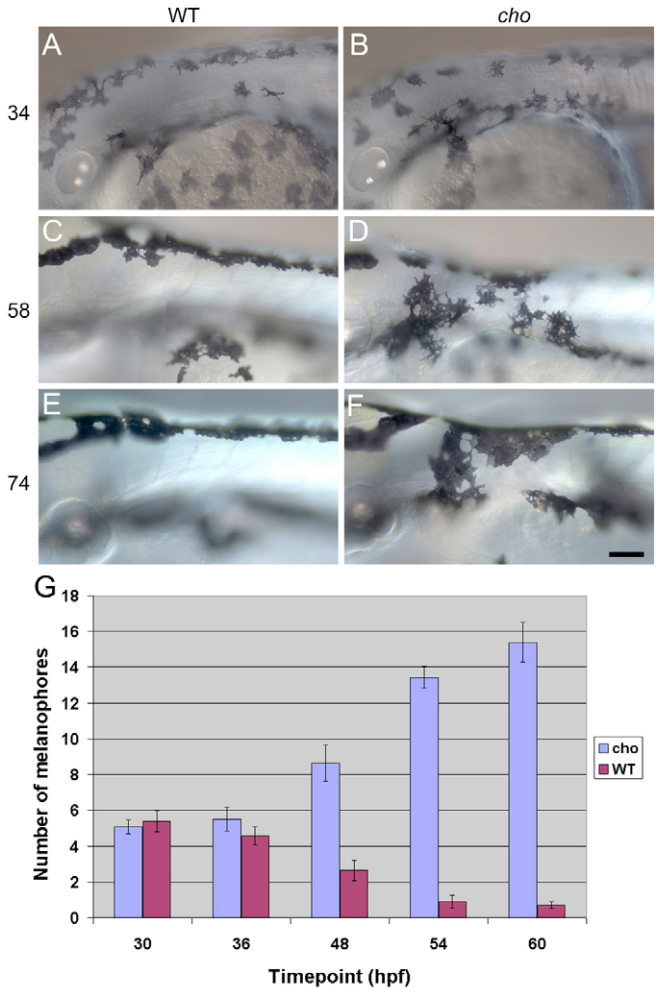

Fig. 1. Timecourse of anterior trunk pigment pattern formation in WT and *cho* mutants during period of collar formation. Lateral views of WT (**A**,**C**,**E**) and *cho* mutant (**B**,**D**,**F**) embryos are shown. Melanophores were seen on the lateral pathway in *cho* mutants and WT siblings at 34 hpf (A,B), and were thereafter absent from WT, but accumulated steadily in *cho* mutants (C-F). Note too the change in collar melanophore morphology between 58 hpf, when their stellate morphology correlated with migratory activity, and 74 hpf, when their more flattened shape reflects a more static phase. Scale bar: 50 μm. (**G**) Total number (means±s.e.) of melanophores on lateral pathway of somites 1-5 throughout collar formation.

formation was confirmed by timelapses starting at 48 hpf, which showed dramatic differences in melanophore behaviour between WT and *cho* mutants (Fig. 2 and see Movies 1 and 2 in the supplementary material). The anterior trunk of WT embryos usually remained entirely devoid of melanophores (Fig. 2A-D). Although melanophores in both dorsal and ventral stripes were highly protrusive and frequently extended processes into the surrounding region, they remained in the dorsal and ventral stripes (Fig. 2I-L). Occasional melanophores were observed in the anterior trunk lateral pathway of a WT at the beginning of the timelapse, but these always migrated rapidly and joined either the ventral or dorsal stripe. Thus, from 48 hpf, WT melanophores exhibited exploratory behaviour but did not migrate through the collar region. By 48 hpf, *cho* mutants had a few melanophores in the nascent collar. These cells were highly active, extending numerous processes, but usually remained

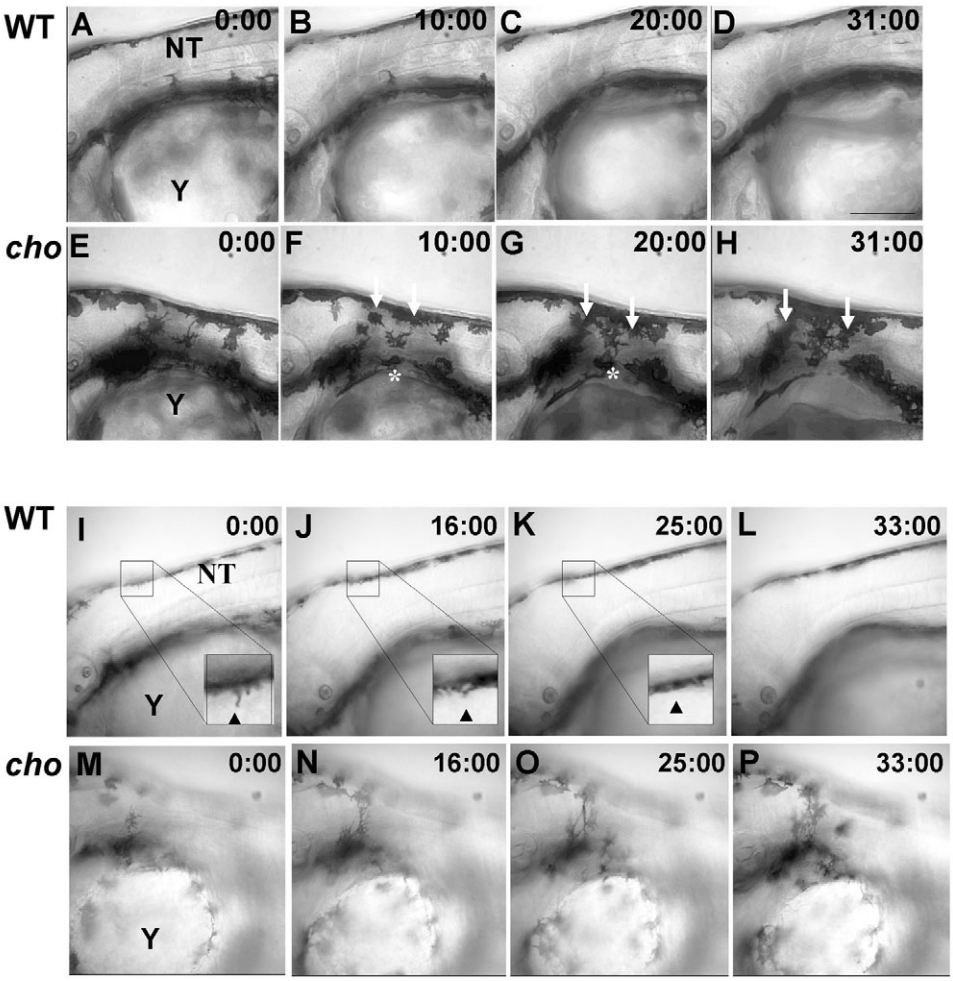

Fig. 2. Timelapse microscopy of 48 hpf WT and *cho* mutants. (**A-H**) Images from different focal planes combined by projection revealed that WT melanophores (A-D) never entered the anterior trunk lateral pathway. By contrast, *cho* mutant melanophores (E-H) invaded the collar, both as single cells from the ventral stripe (asterisk) and as a sheet from the dorsal stripe (arrows). (**I-P**) Images from single focal planes clarify movements of individual cells. WT melanophores (I-L) extend processes into the anterior trunk (arrowhead, I) but these retract (arrow, arrowhead in J,K), whilst *cho* mutant melanophores (M-P) invade the collar, usually remaining ectopically. NT, neural tube; Y, yolk. Scale bar: 150 μm.

stationary and displayed the characteristic radially-symmetric stellate shape of non-migratory melanophores. As in WT siblings, melanophores from both dorsal and ventral stripes of *cho* mutants showed extensive protrusive behaviour exploring the lateral pathway, but unlike WT, these cells frequently migrated into the collar region (Fig. 2E-H,M-P). Thus, *cho* mutant melanophores migrated into the lateral pathway at times when WT melanophores were restricted to one of the pigment stripes. Such behaviour was observed only in the collar region of *cho* mutants.

Derivatives of neural crest cells that migrate on the lateral pathway are consistently defective in *cho* mutants

Anterior trunk NC generates a wide range of derivatives. We used a series of molecular markers to determine which of them, beside melanophores, showed abnormalities in *cho* mutants. Some anterior-most trunk NC contributes to the branchial arches (Schilling and Kimmel, 1994), but Alcian Blue staining revealed no differences in jaw cartilages in 3- and 5-day post-fertilisation (dpf) *cho* mutants and their WT siblings (Fig. 3A,B; data not shown). Likewise, this region generates cardiac NC (Li et al., 2003; Sato and Yost, 2003), but simple observation revealed normal heart morphology, regular heart beat and good blood flow (data not shown).

NC cells migrating on the medial pathway generate neurons and glia of the sensory and sympathetic ganglia, plus melanophores and iridophores. Using incident lighting to detect iridophores, we observed no abnormalities in iridophore number, size or distribution in *cho* mutants (data not shown). Likewise, *foxd3* expression (Kelsh et al., 2000a) revealed no change in glia on the PLL nerve (data not shown), although projection of the nerve itself was aberrant (see below). Immunofluorescent studies using the anti-Hu antibody (Kelsh and Eisen, 2000) revealed that enteric neurons were normal in *cho* mutants (Fig. 3C,D). Similarly, sensory neurons were largely unaffected; the only difference being a slight increase in the number of DRG neurons in the anterior trunk of *cho* mutants at 5 dpf (Fig. 3E-H; Table 1).

Lateral pathway NC cells generate only melanophores and xanthophores. Expression of *GTP cyclohydrolase I* (*gch*) (Parichy et al., 2000b) is an early and persistent marker of the xanthoblast lineage. A *gch* riboprobe in situ hybridisation revealed normally distributed, *gch*-positive cells in 20-hpf *cho* mutants. A gradual clearing of xanthoblasts from the region of the collar, but not from more anterior or posterior regions, was observed in *cho* mutants at subsequent stages beginning at 24 hpf (Fig. 3I-N). By 48 hpf, the collar region was essentially devoid of xanthophores. Taken together with the prominent melanophore collar, it is clear that both NC derivatives utilising the lateral migration pathway display severe defects restricted to the collar region of *cho* mutants.

Collar xanthophore defects in *cho* mutants are causally independent of melanophore defects

In view of the remarkable correlation between the xanthophore and melanophore defects in the collar, we asked whether these pigment cell defects might be causally related. Although our studies

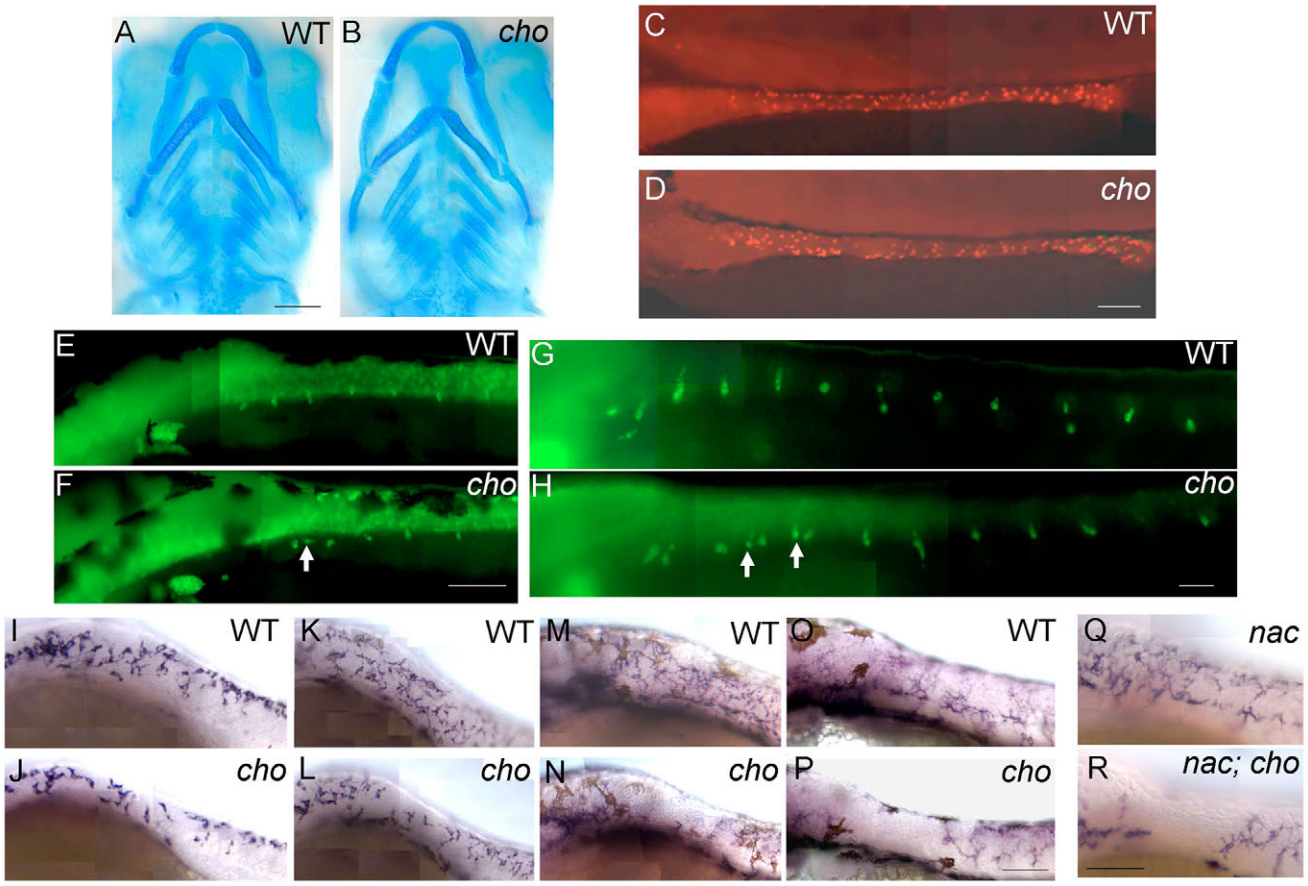

Fig. 3. NC derivatives of lateral, but not medial, migration pathway are defective in *cho* mutants. (**A**,**B**) Alcian Blue staining of craniofacial cartilage in 5 dpf WT (A) and *cho* mutant (B) embryos. (**C-H**) Anti-Hu detection of enteric neurons at 3 dpf in WT (C) and *cho* mutant (D) embryos, and of DRG sensory neurons at 48 hpf (E,F) and 5 dpf (G,H) in WT (E,G) and *cho* mutant (F,H) embryos. As reported previously in WT embryos (An et al., 2002), we observed some ectopic sensory neurons at both 48 hpf and 5 dpf (arrows, F,H; see also Table 1). (**I-P**) In situ hybridisation with *GTP-cyclohydrolase* (*gch*) on WT (I,K,M,O) and *cho* mutants (J,L,N,P) at 24 hpf (I,J), 30 hpf (K,L), 36 hpf (M,N) and 48 hpf (O,P). (**Q**,**R**) 48 hpf. *cho* mutant collar xanthophore defects are independent of melanophores. In situ hybridisation with *gch* showed that whilst *nac* mutants had a WT xanthoblast pattern throughout the trunk (Q), *cho;nac* double mutants still displayed loss of xanthoblasts from the collar region (R). Embryos are shown in lateral view, anterior to the left; except for A,B which are ventral views, anterior up. Scale bars: A,B, 50 μm; C,D,G,H, 75 μm; E,F, 100 μm; I-P, 150 μm; Q,R, 175 μm.

revealed melanophore accumulation beginning after xanthoblast loss, unpigmented precursor cells of the melanophore lineage migrating through this collar region could conceivably drive xanthophore loss. We therefore asked whether xanthophore loss occurred in the absence of melanophores or their precursors using the *nacre* (*nac*) mutant to eliminate the melanophore lineage (Lister et al., 1999). Mutant embryos doubly homozygous for *nac* and *cho* exhibited an additive combination of the loss of *gch*-expressing cells from the collar region as in *cho* mutants, and the absence of all melanophores as in *nac* mutants (Fig. 3Q,R). We conclude that xanthophore loss in *cho* mutants is independent of the melanophore lineage.

cho mutant melanophore abnormalities correlate spatially with defective muscle development

The initial description of *cho* mutants noted a 'hindbrain indentation' correlating with the melanophore collar at 5 dpf (Kelsh et al., 1996). Transverse sections of the collar region identified a

Table 1. Sensory neuron counts in DRGs

	Anterior trunk (segments 1-6)		Posterior trunk (segments 7-14)		Tail	
Genotype	WT	*cho*⁻	WT	*cho*⁻	WT	*cho*⁻
DRG neurons at 48 hpf	11±1.0 *n*=10	11±0.72 *n*=14	13±1.3 *n*=4	15±2.2 *n*=4	–	–
Ectopic DRG neurons at 48 hpf	0.20±0.20 *n*=10	0.71±0.19 *n*=14	–	–	–	–
DRG neurons at 5 dpf	38.5±1.43 *n*=10	45.9±2.06* *n*=10	35.2±2.00 *n*=10	39.3±1.70 *n*=10	79.5±2.95 *n*=10	74.6±1.55 *n*=10
Ectopic DRG neurons at 5 dpf	2.30±0.47 *n*=10	3.30±1.12 *n*=10	0.50±0.22 *n*=10	0.70±0.70 *n*=10	4.90±0.98 *n*=10	5.60±1.42 *n*=10

Counts are shown as mean±s.e.m.
*$P<0.01$, Student's *t*-test.

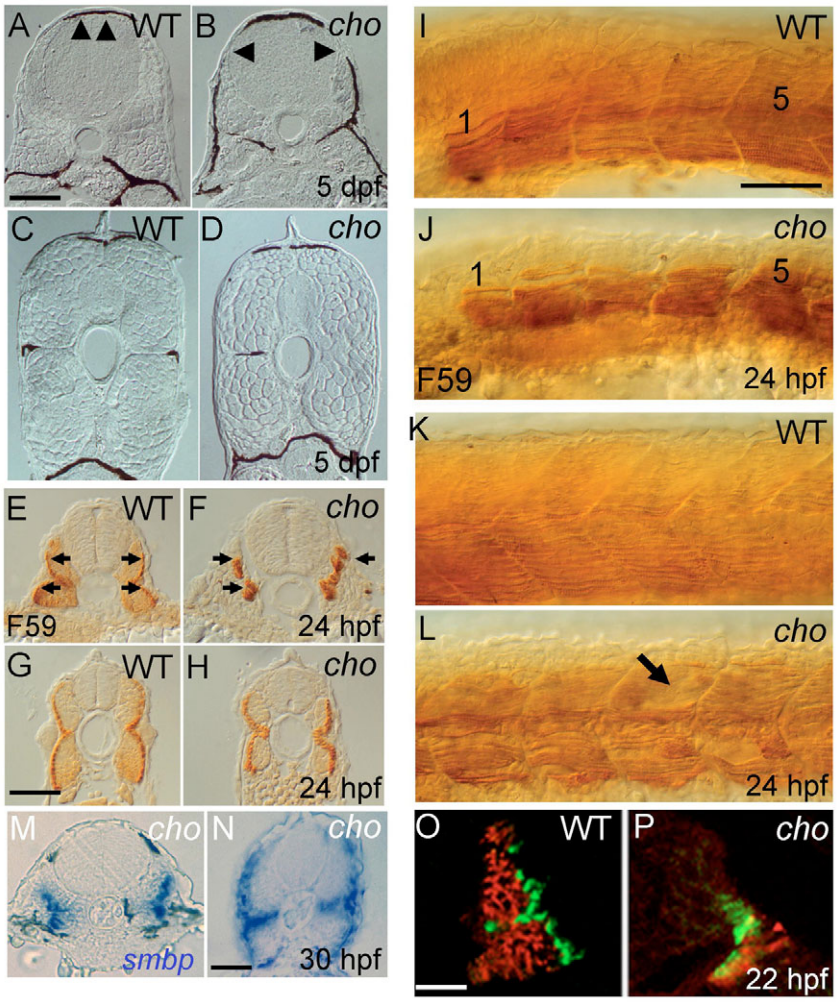

Fig. 4. Somite defects in *cho* mutants. (**A-D**) Transverse sections of 5 dpf embryos reveal defective muscle block extension in anterior (arrowheads, A,B), but not posterior (C,D), trunk of *cho* mutants (B,D) as compared with WT (A,C). *cho* mutants typically lack melanophores and horizontal myoseptum; exceptionally, as here (left side), a single melanophore may be present, but in an abnormal position. (**E-H**) Sections of anterior (E,F) and posterior (G,H) trunk of 24 hpf WT (E,G) and *cho* mutant (F,H) embryos labelled with F59 antibody to show slow muscle fibres (arrows in E,F). (**I-L**) Lateral view of anterior (I,J; somites 1 and 5 indicated) and posterior (K,L) trunk of 24 hpf WT (I,K) and mutant (J,L) embryos labelled with F59 antibody; note the disorganised slow muscle fibres and apparent holes in fibre pattern (arrow) in *cho* mutant. (**M**,**N**) Transverse sections of anterior (M) and posterior (N) trunk of 30 hpf *cho* mutant showing *smbp* RNA in situ hybridisation. (**O**,**P**) At the 26-somite stage, WT somites (O) consist largely of fast muscle (red; antibody EB165) under surface slow muscle (green; BAD5), whereas *cho* mutants (P) displayed severely decreased fast muscle. Scale bars: A-D,I-L, 75 μm; E-H, 25 μm; M,N, 40 μm; O,P, 25 μm.

defect in dorsal extension of the myotome causing this dorsoventral flattening (Fig. 4A-D). Immunohistochemistry using F59 revealed disorganisation of slow muscle fibres in the anterior somites (Fig. 4I-L). Transverse sections showed that these anterior-most *cho* mutant somites had abnormally positioned slow fibres, with these fibres located medially in the myotome (Fig. 4F). By contrast, slow muscle was found peripherally in posterior trunk somites of *cho* mutants and at all axial levels in WT siblings (Fig. 4E,G,H). To address the time of onset of slow muscle defects, we examined stage-specific markers of slow muscle differentiation. Slow myosin binding protein (Smbp; P.D.C., unpublished), is absent from migratory slow fibres, but expressed within differentiated muscle pioneer cells (MPs) (Ekker et al., 1992) and post-migratory surface slow muscle. RNA in situ hybridisation with *smbp* confirmed the defect in radial migration of slow muscle cells (Fig. 4M,N), and indicated that slow muscle cells had differentiated on schedule. In situ hybridisation of 16-18 hpf *cho* mutants and WT with a specific marker for pre-migratory slow muscle precursor cells (*prox1*) (Glasgow and Tomarev, 1998) showed that *cho* mutants were indistinguishable from WT prior to migration of slow muscle progenitors (data not shown). Furthermore, there was no alteration in the expression of adaxial cell markers such as *ptc1* and *myod*, suggesting that the initial Hedgehog-dependent specification of these cells was unaltered in *cho* mutant homozygotes. In situ hybridisation with an *engrailed* probe, as well as the anti-Engrailed antibody 4D9, to identify MPs showed that *cho* mutants possess MPs at 24 hpf and 30 hpf. *cho* mutant MPs were morphologically indistinguishable from those of WT at 24 hpf, but showed reduced labelling by 30 hpf, consistent with the general reduction in all fibre types at this stage (data not shown). Collectively, these analyses suggest that the initial specification and differentiation of muscle cells is unaltered within the anterior myotomes of *cho* mutants, whereas the subsequent morphogenesis of these cells is altered within mutants. As expected, given the aberrant distribution of slow muscle, fast muscle fibres were also abnormally organised, but in addition were clearly reduced in number (Fig. 4O,P). Counts of both fast and slow muscle fibres labelled with anti-MyHc (myosin heavy chain) antibody in transverse sections showed that the number of both types of fibres was reduced in anterior myotomes of *cho* mutants to less than 50% of those present in WT siblings (data not shown). Examination of embryos labelled with anti-MyHc antibody showed progressive fibre loss through the embryonic and larval period (see Fig. S1 and Movies 3 and 4 in the supplementary material). In contrast to the migration defect, this quantitative aspect of the slow muscle phenotype extended beyond the anterior-most myotomes, but was strongest anteriorly and absent in the posterior-most trunk (Fig. 5). Confocal 3D reconstruction revealed that individual muscle fibres frequently failed to span the entirety of the myotome (see Movie 5 in the supplementary material). Therefore, the decreased fibre number evident in transverse sections is likely to result from fibre loss through fibre detachment as well as reduction in overall initial fibre number.

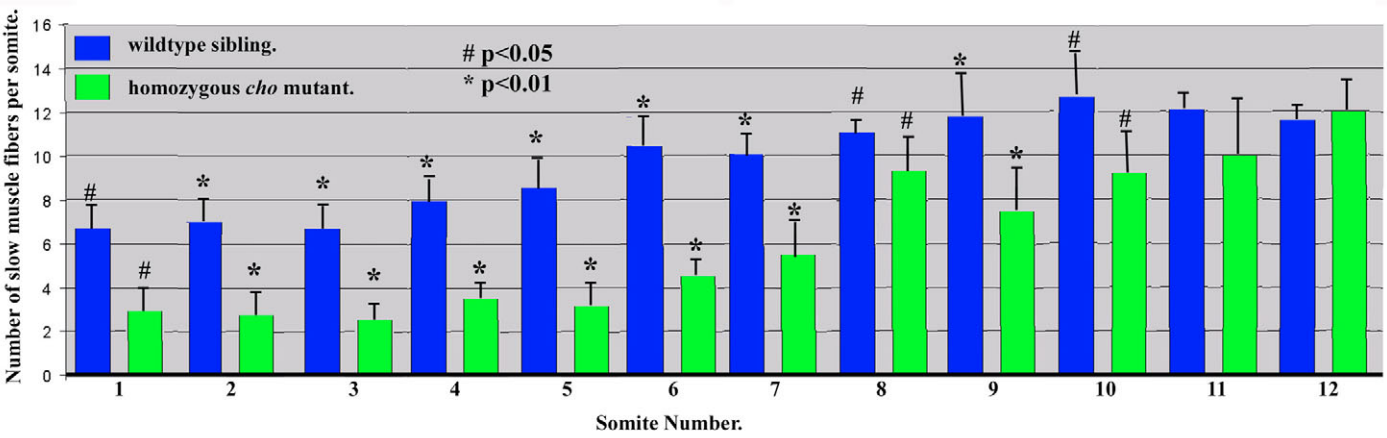

Fig. 5. Quantitation of slow muscle fibre numbers at different axial positions at 30 hpf. Student's *t*-test *P* values for comparisons between *cho* and WT are indicated. Mean±s.d.; *n*=4.

Together these results reveal a complex myotomal phenotype in the anterior-most trunk of *cho* mutants. The abundance of all muscle fibre types is strongly reduced and migration, but not differentiation, of slow muscle cells is severely compromised. The resultant, greatly altered architecture of anterior myotomes later includes a lack of dorsal extension of the myotome and muscle fibre loss through a process of detachment. However, myotome architecture also shows defects (e.g. fibre detachment) in the posterior trunk, suggesting that the melanophore collar phenotype is not simply a consequence of abnormal myotomal structure.

Ectopic migration of melanophores in *cho* mutants results from defective somite development

Using somite transplantation, we tested whether the defective somite development of *cho* mutants underlies melanophore collar formation. We transplanted WT anterior somites into *cho* mutant hosts or WT sibling controls after extirpation of the host somite. The donor tissue was marked by GFP from a skeletal muscle-specific promoter. Transplants were performed isochronically at 24 hpf and monitored during the next 4 days for collar formation. Transplanted somites expressed GFP under control of the alpha actin promoter at similar levels and timing as non-transplanted somites; expression of the transgene was maintained throughout the period the transplanted larvae were raised. As shown in other contexts (Bassett et al., 2003), the activation and maintenance of the alpha actin-GFP transgene is a sensitive indicator of muscle integrity. Thus, muscle differentiation appeared normal within the transplant. Further analysis of the integrity of muscle within the transplant was monitored by differential interference contrast (DIC) optics, to assay the presence of intact sarcomeric arrays within fibres. Sarcomeric assembly appeared normal in the transplanted somites, suggesting that muscle differentiated and was maintained normally within transplanted tissue. Melanophores freely traversed the transplanted tissue at early developmental time points both in WT → WT (*n*=17) and WT → *cho* mutant (*n*=6) transplants (Fig. 6D-F). However, by 72 hpf, melanophores were excluded from the regions lying directly above transplanted WT somites in *cho* mutants (6 out of 6). By contrast, they collected freely at other locations lacking WT tissue, such as within the collar region adjacent to the transplant, as well as on the contralateral side of the embryo (Fig. 6A-C). No defect in melanophore migration or patterning was seen within control WT → WT transplants (17 of 17). This shows that the *cho* mutant somites cause the mispatterning of melanophores to form the collar.

Abnormally distributed *sdf1a* correlates with pigment cell pattern defects in *cho* mutants

As previously reported (David et al., 2002; Li et al., 2004), *sdf1a* is expressed at the horizontal myoseptum in WT embryos but not in *you*-type mutants. *cho* mutants lack *sdf1a* expression along the horizontal myoseptum but have ectopic *sdf1a* over the anterior somites in the collar region (Fig. 7A-C,E). This pattern of expression initiates at 24 hpf and persists through to at least 55 hpf, coinciding with the time of melanophore collar formation. Expression of *sdf1a* is localised to the lateral surface of the somite, adjacent to the lateral NC migration pathway, in a subpopulation of external cells (Devoto et al., 2006; Groves et al., 2005; Waterman, 1969). Thus, in embryos labelled both for *sdf1a* and with MF20 antibody, the *sdf1a*-expressing cells were clearly seen to lie immediately lateral to the MF20-staining myotomal populations (Fig. 7D). In the *you*-type mutants *smu* (*smo* – Zebrafish Information Network) and *con* (*disp1* – Zebrafish Information Network), absence of *sdf1a* in the horizontal myoseptum results in misrouting of the PLL nerve to the ventral domain of *sdf1a* expression (David et al., 2002; Li et al., 2004). By contrast, in *cho* mutants, the PLL primordium was found to migrate dorsally over the ectopic *sdf1a*-expressing collar region, as shown using acetylated alpha tubulin as a PLL nerve marker at 5 dpf (Fig. 8A,B). or the PLL primordium marker *cxcr4b* at 36 hpf (Fig. 8C,D).

Sdf1 is a chemoattractant for melanophores

The altered pattern of *sdf1a* expression in *cho* mutants corresponds to both melanophore patterning defects. To test whether Sdf1 is a chemoattractant for migrating melanophores. We placed beads soaked in recombinant human SDF1 protein against the epidermis of WT embryos, and analysed their effect on melanophore localisation. In cases in which SDF1-soaked beads remained attached to embryos for at least 16 hours during melanophore migration, melanophores accumulated at the location adjacent to the bead (7 of 9) (Fig. 9). By contrast, melanophores never accumulated next to control beads (7 out of 7; data not shown). We note that beads placed on the posterior trunk, at least as posterior as the vicinity of the thirteenth somite, readily attracted melanophores (Fig. 9C-E). The integrity of muscle adjacent to the transplant was checked by

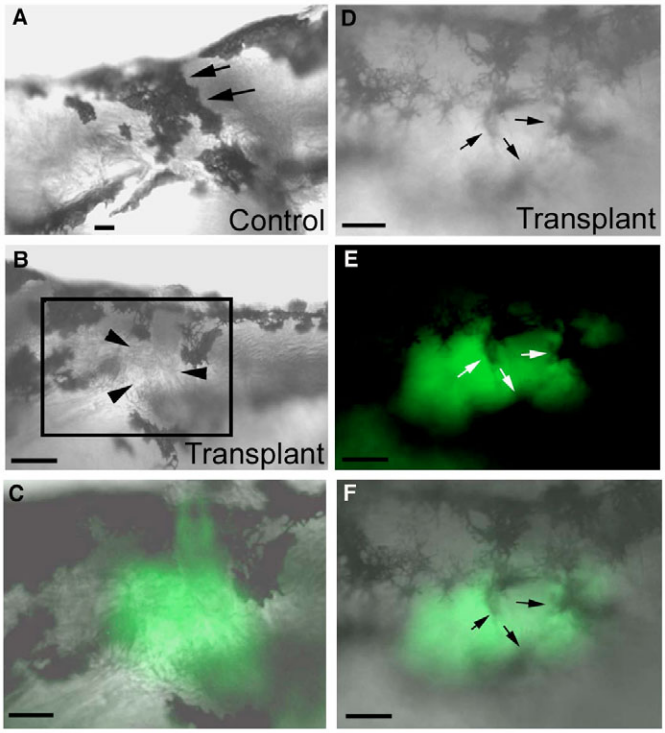

Fig. 6. The *cho* mutant melanophore collar defects are caused by an underlying somite defect. (**A-C**) WT → *cho* mutant somite transplant embryo. (A) Right-hand, non-transplanted control side of a *cho* homozygote showing the melanophore collar at 5 dpf (arrows). Dorsal is to the top, anterior to the right. (B) Left-hand, experimental, transplanted side of the same embryo at the same time as in A. Note the gap in the collar on this side (arrowheads). (C) High magnification of boxed region in B, showing tight correlation of transplanted WT somite from alpha actin-GFP donor (green) with the collar region avoided by melanophores. Anterior is to the left, dorsal to the top. (**D-F**) The same transplanted WT → *cho* chimaeric embryo at 24 hours post-transplantation (2 dpf), showing that at early stages melanophores (arrows) traverse the transplanted tissue freely. Lateral views, anterior to the left, dorsal to the top. (D) Collar region on experimental side showing multiple melanophores traversing the transplant. (E) Fluorescent image showing the WT transplanted tissue (green). (F) D and E merged. Scale bars: 130 μm in B; 60 μm in A,C-F.

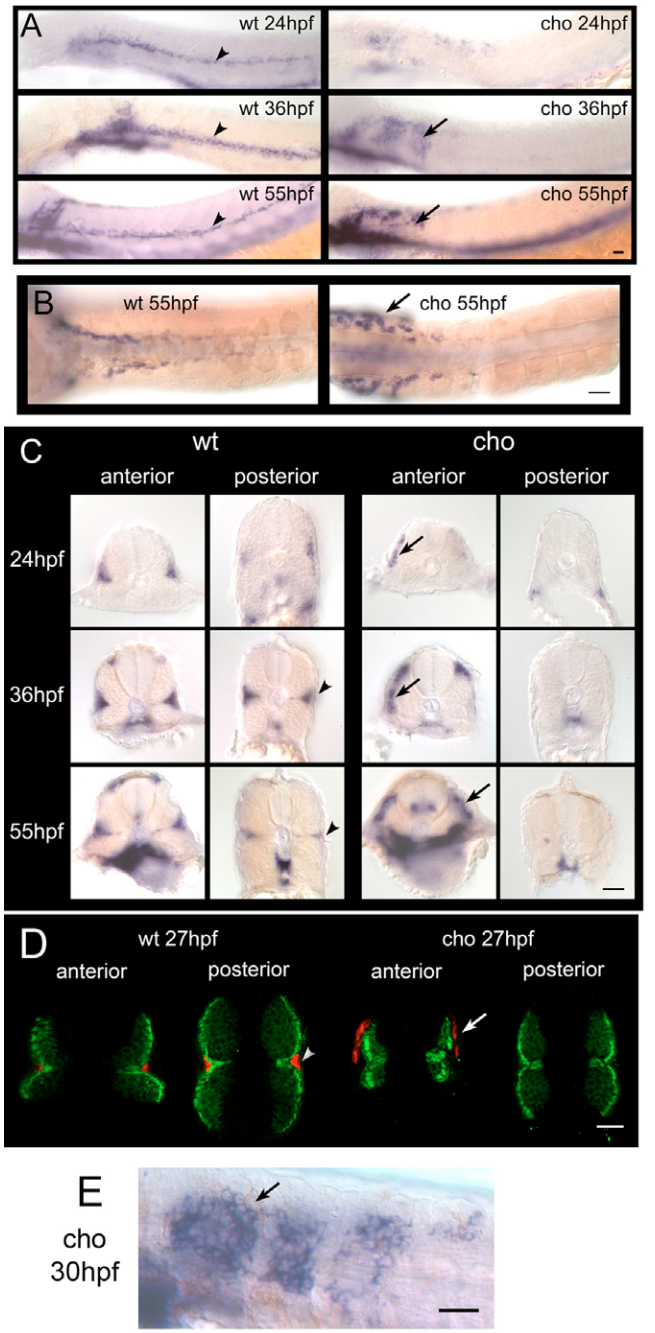

Fig. 7. *sdf1a* whole-mount mRNA in situ hybridisations in WT and *cho* mutant. *sdf1a* is expressed in disk-shaped somite external cells along the horizontal myoseptum (arrowheads) in WT and in the collar region (arrows) in *cho* mutants. (**A**) Lateral views at 24, 36 and 55 hpf. (**B**) Dorsal views at 55 hpf. (**C**) Transverse cross-sections through the anterior and posterior trunk at 24, 36 and 55 hpf. (**D**) Confocal images of transverse cross-sections through the anterior and posterior trunk at 27 hpf showing superficial expression of *sdf1a* mRNA (red) compared with MF20 antibody staining of muscle (green). (**E**) Higher magnification lateral view of *cho* anterior trunk at 30 hpf. Scale bars: 25 μm.

serial sectioning of bead-implanted embryos and staining with anti-MyHc antibody to determine if muscle differentiation and maintenance were affected. In all cases, muscle adjacent to the bead appeared normal (n=5); a representative section containing ectopic melanophores immunolabelled for MyHc is illustrated (Fig. 9E). Implanted animals were also monitored using DIC optics to analyse fibre integrity, which also appeared normal. We then placed SDF1-soaked beads on *cho* mutant embryos at various locations in the trunk and tail. As in WT embryos, ectopic melanophores accumulated adjacent to the bead (10 of 14) (Fig. 9F). Thus, in both WT and *cho* mutant embryos, ectopic SDF1 can act as a chemoattractant for melanophores throughout the entire trunk.

Sdf1a knock-down reduces the *cho* mutant melanophore collar and the WT lateral stripe

To test whether altered Sdf1a expression could account for each of the melanophore defects in *cho* mutants (Fig. 10A), we used morpholino oligonucleotide injection to attenuate its activity. At 55 hpf, morpholino-injected *cho* mutants showed only 54% of the number of collar melanophores of uninjected *cho* mutant siblings. Likewise, in the WT siblings, those injected with *sdf1a*

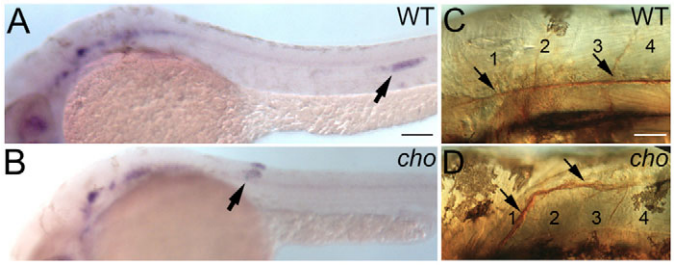

Fig. 8. Abnormal primordium migration results in misrouting of the PLL nerve in anterior-most trunk of *cho* mutant embryos. (**A**,**B**) Whole-mount mRNA in situ hybridisation of *cxcr4b* in 34 hpf WT (A) and *cho* mutant (B) to show aberrant migration of PLL primordium (arrow). (**C**,**D**) This results in misrouting and truncation of PLL nerve (arrow), as seen by zn-12 immunohistochemistry on 56 hpf WT (C) and *cho* mutant (D) embryos. Somites are numbered. Scale bars: 50 μm in A,B; 20 μm in C,D.

morpholino showed only 45% of the number of lateral stripe melanophores as compared with the uninjected controls (Fig. 10B).

We conclude that invasion of melanophores to form the ectopic collar is at least in part driven by ectopic Sdf1a expression in the collar region. Also, WT lateral stripe patterning is at least partly dependent on *sdf1a* expression by cells adjacent to the horizontal myoseptum, and that absence of this expression in *cho* mutants contributes to the absence of the lateral stripe.

DISCUSSION

Sdf1 and the control of pigment pattern in zebrafish

Our demonstration that the lateral neural crest migration pathway is closed down at a specific time in normal development, thus preventing invasion by melanophores of the adjacent nascent dorsal and ventral stripes, is the first indication that closure of this migration pathway is important for pigment pattern maintenance. These observations complement earlier work showing that opening of the pathway is also tightly regulated (Jesuthasan, 1996). The latter study indicated that NC cell invasion of the lateral pathway is delayed by an inability of the substrate to support cell adhesion and traction. Here, we have shown that a similar incompatibility of substrate and pigment cells is reasserted around 36 hpf. Interestingly, this constraint is overcome in *cho* mutants, at least in part owing to the ectopic expression of Sdf1a.

We have demonstrated a role for Sdf1a in *cho* mutant collar and normal lateral stripe formation. Notably, *sdf1a* expression is not disrupted in anterior somites in other *you*-type mutants examined (David et al., 2002) (data not shown), consistent with this being a key feature driving the unique collar pigmentation of *cho* mutants. In the case of germ cell and PLL primordium migration, Sdf1a expression acts as a 'roadway' constraining the migrating cells to a specific route (Doitsidou et al., 2002; Knaut et al., 2003; Schier, 2003). Nevertheless, in both systems, ectopic expression of the ligand has established that redirection of both germ cell and PLL primordium migration can occur at a distance (Doitsidou et al., 2002; Knaut et al., 2003; Li et al., 2004). Which of these mechanisms is most important for lateral stripe formation is unclear, as the migration route taken by lateral stripe melanoblasts is still poorly defined. Although our data suggest a role for Sdf1a signalling in lateral stripe formation, other aspects of the WT melanophore pattern do not show a correlation with *sdf1a* expression and are

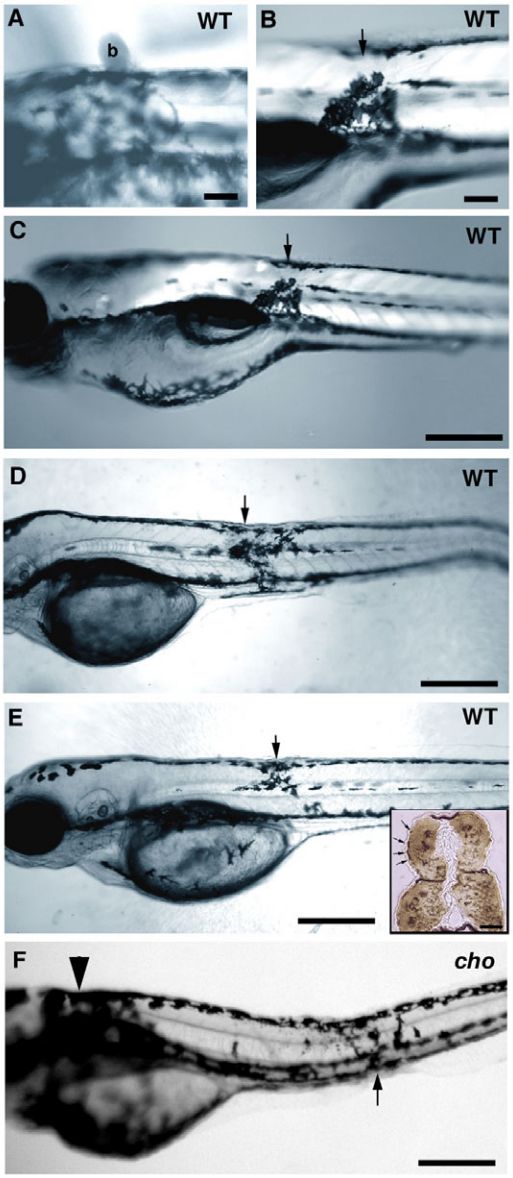

Fig. 9. Implantation of Sdf1-soaked beads into WT and *cho* mutant embryos results in the formation of an ectopic melanophore collar. (**A**) SDF1-soaked beads (b) were implanted in a dorsal position directly against the skin of a WT embryo at 24 hpf, held in place by a drop of low melting point agarose. Embryos were photographed at 48 hpf to ensure the bead had stayed in place and to record the location of the bead. Agarose holding the bead distorts light transmission, causing the halo evident in this image. (**B**) Same embryo as in A but at 72 hpf, after bead removal to document the phenotype. The position at which the bead was placed is marked with an arrow. Melanophores have accumulated ectopically, adjacent to the location of the bead implant. (**C**) Low magnification of same larva as in B. (**D**,**E**) Two independent WT embryos, treated similarly, also show ectopic melanophore accumulations adjacent to the location of the SDF1 bead (arrows). Ectopic melanophores form regardless of where in the embryo the bead is positioned. Insert in E is the same animal sectioned in an area containing ectopic melanophores, immunolabelled for MyHc (brown) and demonstrating that bead implantation did not affect muscle differentiation or maintenance. Note that beads are not surgically implanted, but merely placed on the skin; thus, no wound is formed. (**F**) Implantation of SDF1 beads in homozygous *cho* mutant embryos (note collar, arrowhead) results in similar accumulation of ectopic melanophores adjacent to site of bead (arrow). Scale bars: 100 μm in A,B; 350 μm in C-F; 25 μm in insert.

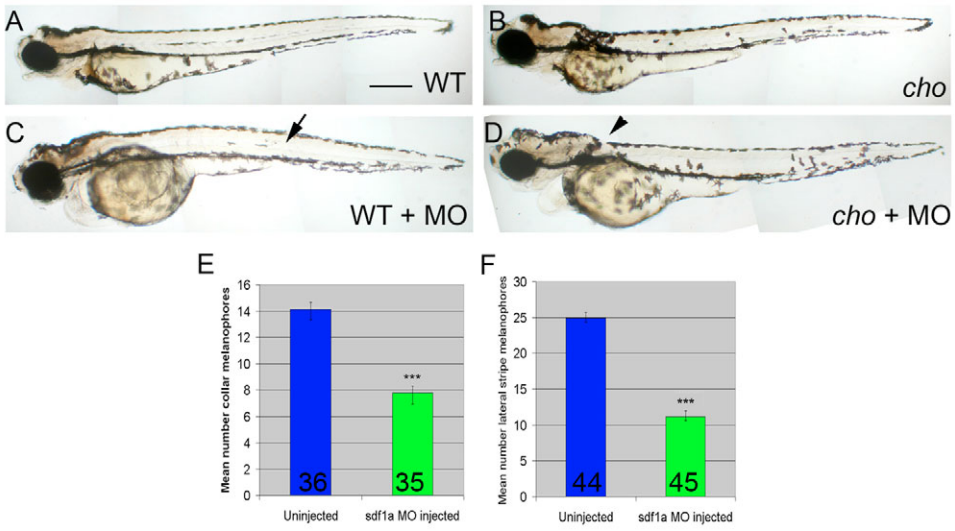

Fig. 10. Morpholino-mediated knock-down of *sdf1a* generates melanophore patterning defects in 55 hpf embryos. (**A-D**) Fixed *cho* mutant embryos (B,D) and WT siblings (A,C) with (C,D) or without (A,B) *sdf1a* morpholino. Note the decreased numbers of melanophores in the WT lateral stripe (arrow) and the *cho* collar (arrowhead) after morpholino injection. Scale bar: 375 μm. (**E**,**F**) Quantitation of these defects. (E) Lateral pathway collar melanophores of *cho* mutant embryos. (F) Lateral stripe melanophores of WT siblings. Bar graphs show mean±s.e. melanophore counts per embryo; number of embryos is indicated at base of bar. WT and *cho* mutants were identified by their anterior trunk myotome phenotypes. Reduction of *cho* mutant collar and WT lateral stripe melanophores were both highly significant; ***, Student's *t*-test $P<0.0001$.

likely to be independently controlled. Consistent with this, both dorsal and ventral stripe melanophores are unaffected in *sdf1a* morphants (data not shown).

In other contexts documented to date, Sdf1a function has been shown to be mediated by Cxcr4b. We were thus surprised to find that expression of neither of the known Sdf1a receptor genes, *cxcr4a* and *cxcr4b*, can be detected in any pigment cells in WT or *cho* mutants (S.E. and P.W.I., unpublished). This may be due to sub-detection-threshold expression levels in melanophores, or even persistent Cxcr4a protein, as *cxcr4a* expression is seen in premigratory NC cells (Chong et al., 2001). However, initial studies of *cxcr4a* morphants do not reveal any melanophore patterning defect (T.R.C. and R.N.K., unpublished). Moreover, we have been unable to identify any other *cxcr4*-like genes in the zebrafish genome. One possibility is that the effects of Sdf1a are mediated by a novel Sdf1 receptor in pigment cells. Consistent with this proposition is the demonstration that an orphan receptor, RDC1 (CXCR7 – Human Gene Nomenclature Database), is responsible for SDF1 signalling in human T lymphocytes (Balabanian et al., 2005). Finally, Sdf1a might act only indirectly in melanophore patterning via its effects on another cell type, as shown in other contexts. For example, migration of the PLL nerve sensory afferent growth cones along the horizontal myoseptum is dependent upon Cxcr4b-Sdf1a signalling, yet elegant analyses of genetic chimaeras demonstrate that the guidance cues act on the PLL primordium which migrates ahead of these growth cones and tows them along (Gilmour et al., 2004). Further work to identify the precise mechanism whereby Sdf1a influences melanophores will now be paramount.

It is notable that whilst *cho* mutants have a profound effect on lateral pathway migration, the effects on the medial pathway are at most minor. The identification of ectopic *sdf1a* expression as an underlying cause of the collar phenotype helps clarify this, as the ectopic *sdf1a* expression is localised only to the lateral face of the developing somite. It is therefore likely that NC cells utilising the medial pathway are largely shielded from this influence. Furthermore, a recent study identified cells of the slow muscle lineage as a key guidance cue for medial pathway NC migration (Honjo and Eisen, 2005). Since slow muscle fibres initially form normally and show regular organisation in the majority of somites in *cho* mutants, it is perhaps not unexpected that medial pathway NC migration is normal.

cho mutants show more severe somite defects anteriorly than posteriorly

Some aspects of the *cho* mutant phenotype affect somites along the whole anterior-posterior axis, including the U-shaped appearance and detachment of many muscle fibres from vertical myosepta. By contrast, some defects, such as ectopic *sdf1a* expression, lack of somite dorsal extension and slow muscle migration, only affect the anterior-most five somites. These defects are likely to be an autonomous property of anterior somitic cells of *cho* mutants, as WT tissue transplanted into *cho* mutants does not develop similar structural defects as the surrounding *cho* mutant tissue.

There are other examples of anterior somites behaving differently to more-posterior somites, including mutants in which only more-posterior somites are affected (van Eeden et al., 1996). Indeed, adaxial cell specification might be regulated by distinct signalling pathways in anterior and posterior somites; for instance, pertussis toxin-mediated manipulation of intracellular signalling pathways is reported to result in defects restricted to posterior somites (Hammerschmidt and McMahon, 1998). Furthermore, recent observations suggest that cell adhesion systems may also be differentially deployed in anterior and posterior somites, as mutations in *integrin alpha 5* alter segmentation of only the first seven somites (Julich et al., 2005). These observations are particularly intriguing in relation to the *cho* mutant muscle detachment phenotype.

cho mutants differ from other *you*-type mutants

Although traditionally grouped with the *you*-type mutants owing to its U-shaped somites and weak myoseptal phenotype, *cho* has been proposed to act downstream of the other *you*-type genes in the

somite development pathway (van Eeden et al., 1996). Our characterisation of the *cho* mutant muscle phenotype reveals extensive differences from the *you*-type group, e.g. general myotome disruption including both slow and fast muscle and retention of muscle pioneer cells. We propose that *cho* does not strictly belong to the *you*-type gene class and that the shared somite shape phenotype may be caused by different mechanisms. Molecular characterisation of the *cho* locus may illuminate this. The *cho* mutation has been mapped to a crucial region but is not yet identified. Interestingly, we have been unable to identify genes encoding known components of the SDF signaling pathway in this crucial region (G.E.H. and P.D.C., unpublished).

In summary, the studies reported here demonstrate the nature of the myotomal and pigment patterning defects evident in the *cho* mutant, defining a novel phenotype distinct from the *you*-type mutant class to which *cho* was initially assigned. Analysis of this phenotype has revealed that misregulation of the chemokine Sdf1a within the myotome is a key causative factor in the melanophore patterning defects of *cho* homozygotes. This is significant because, for the first time, it implicates the Sdf1-mediated signal transduction pathway in pigment pattern formation. It will be of interest now to determine how widely this patterning mechanism is used to control the patterning of NC derivatives throughout the vertebrate clades.

We thank John James, Kim Denny, Leanne Price, Richard Squire, David Keenan, Julian Cocks, Fiona Browne and Lisa Gleadall for expert fish care; Ruth Bremiller and Michelle McDowel for plastic and cryostat sectioning; David Parichy for the *gch* probe, Alain Ghysen for the *sdf1a* probe and Sam England for the *eng* probe. We also thank members of the R.N.K. and P.D.C. laboratories for excellent suggestions during the course of this work. This work was funded by MRC Co-operative Group Grant G9721903 (to R.N.K.), University Postgraduate Studentship and ORS award (to V.N.), Howard Florey Fellowship (to G.E.H.), MRC programme grant G0100151 (to P.W.I.) and NIH Grant HD22486 (to J.S.E.).

Supplementary material

Supplementary material for this article is available at
http://dev.biologists.org/cgi/content/full/134/5/1011/DC1

References

An, M., Luo, R. and Henion, P. D. (2002). Differentiation and maturation of zebrafish dorsal root and sympathetic ganglion neurons. *J. Comp. Neurol.* **446**, 267-275.

Asai, R., Taguchi, E., Kume, Y., Saito, M. and Kondo, S. (1999). Zebrafish leopard gene as a component of the putative reaction-diffusion system. *Mech. Dev.* **89**, 87-92.

Balabanian, K., Lagane, B., Infantino, S., Chow, K. Y., Harriague, J., Moepps, B., Arenzana-Seisdedos, F., Thelen, M. and Bachelerie, F. (2005). The chemokine SDF-1/CXCL12 binds to and signals through the orphan receptor RDC1 in T lymphocytes. *J. Biol. Chem.* **280**, 35760-35766.

Barresi, M. J., Stickney, H. L. and Devoto, S. H. (2000). The zebrafish slow-muscle-omitted gene product is required for Hedgehog signal transduction and the development of slow muscle identity. *Development* **127**, 2189-2199.

Bassett, D. I., Bryson-Richardson, R. J., Daggett, D. F., Gautier, P., Keenan, D. G. and Currie, P. D. (2003). Dystrophin is required for the formation of stable muscle attachments in the zebrafish embryo. *Development* **130**, 5851-5860.

Blagden, C. S., Currie, P. D., Ingham, P. W. and Hughes, S. M. (1997). Notochord induction of zebrafish slow muscle mediated by Sonic hedgehog. *Genes Dev.* **11**, 2163-2175.

Chong, S. W., Emelyanov, A., Gong, Z. and Korzh, V. (2001). Expression pattern of two zebrafish genes, cxcr4a and cxcr4b. *Mech. Dev.* **109**, 347-354.

Crow, M. T. and Stockdale, F. E. (1986). Myosin expression and specialization among the earliest muscle fibers of the developing avian limb. *Dev. Biol.* **113**, 238-254.

Currie, P. D. and Ingham, P. W. (1996). Induction of a specific muscle cell type by a hedgehog-like protein in zebrafish. *Nature* **382**, 452-455.

David, N. B., Sapede, D., Saint-Etienne, L., Thisse, C., Thisse, B., Dambly-Chaudiere, C., Rosa, F. M. and Ghysen, A. (2002). Molecular basis of cell migration in the fish lateral line: role of the chemokine receptor CXCR4 and of its ligand, SDF1. *Proc. Natl. Acad. Sci. USA* **99**, 16297-16302.

Davies, J. A., Cook, G. M. W., Stern, C. D. and Keynes, R. J. (1990). Isolation from chick somites of a glycoprotein fraction that causes collapse of dorsal root ganglion growth cones. *Neuron* **4**, 11-20.

Devoto, S. H., Melancon, E., Eisen, J. S. and Westerfield, M. (1996). Identification of separate slow and fast muscle precursor cells in vivo, prior to somite formation. *Development* **122**, 3371-3380.

Devoto, S. H., Stoiber, W., Hammond, C. L., Steinbacher, P., Haslett, J. R., Barresi, M. J., Patterson, S. E., Adiarte, E. G. and Hughes, S. M. (2006). Generality of vertebrate developmental patterns: evidence for a dermomyotome in fish. *Evol. Dev.* **8**, 101-110.

Doitsidou, M., Reichman-Fried, M., Stebler, J., Koprunner, M., Dorries, J., Meyer, D., Esguerra, C. V., Leung, T. and Raz, E. (2002). Guidance of primordial germ cell migration by the chemokine SDF-1. *Cell* **111**, 647-659.

Dumstrei, K., Mennecke, R. and Raz, E. (2004). Signaling pathways controlling primordial germ cell migration in zebrafish. *J. Cell Sci.* **117**, 4787-4795.

Ekker, M., Wegner, J., Akimenko, M. and Westerfield, M. (1992). Coordinate embryonic expression of three zebrafish engrailed genes. *Development* **116**, 1001-1010.

Feng, Y., Broder, C. C., Kennedy, P. E. and Berger, E. A. (1996). HIV-1 entry cofactor: functional cDNA cloning of a seven-transmembrane, G protein-coupled receptor. *Science* **272**, 872-877.

Gilmour, D., Knaut, H., Maischein, H. M. and Nusslein-Volhard, C. (2004). Towing of sensory axons by their migrating target cells in vivo. *Nat. Neurosci.* **7**, 491-492.

Glasgow, E. and Tomarev, S. I. (1998). Restricted expression of the homeobox gene prox 1 in developing zebrafish. *Mech. Dev.* **76**, 175-178.

Groves, J. A., Hammond, C. L. and Hughes, S. M. (2005). Fgf8 drives myogenic progression of a novel lateral fast muscle fibre population in zebrafish. *Development* **132**, 4211-4222.

Haffter, P., Granato, M., Brand, M., Mullins, M., Hammerschmidt, M., Kane, D., Odenthal, J., van Eeden, F., Jiang, Y., Heisenberg, C. et al. (1996). The identification of genes with unique and essential functions in the development of the zebrafish, Danio rerio. *Development* **123**, 1-36.

Haines, L., Neyt, C., Gautier, P., Keenan, D. G., Bryson-Richardson, R. J., Hollway, G. E., Cole, N. J. and Currie, P. D. (2004). Met and Hgf signaling controls hypaxial muscle and lateral line development in the zebrafish. *Development* **131**, 4857-4869.

Hammerschmidt, M. and McMahon, A. P. (1998). The effect of pertussis toxin on zebrafish development: a possible role for inhibitory G-proteins in hedgehog signaling. *Dev. Biol.* **194**, 166-171.

Honjo, Y. and Eisen, J. S. (2005). Slow muscle regulates the pattern of trunk neural crest migration in zebrafish. *Development* **132**, 4461-4470.

Imitola, J., Raddassi, K., Park, K. I., Mueller, F. J., Nieto, M., Teng, Y. D., Frenkel, D., Li, J., Sidman, R. L., Walsh, C. A. et al. (2004). Directed migration of neural stem cells to sites of CNS injury by the stromal cell-derived factor 1alpha/CXC chemokine receptor 4 pathway. *Proc. Natl. Acad. Sci. USA* **101**, 18117-18122.

Jesuthasan, S. (1996). Contact inhibition/collapse and pathfinding of neural crest cells in the zebrafish trunk. *Development* **122**, 381-389.

Johnson, S. L., Africa, D., Walker, C. and Weston, J. A. (1995). Genetic control of adult pigment stripe development in zebrafish. *Dev. Biol.* **167**, 27-33.

Julich, D., Geisler, R. and Holley, S. A. (2005). Integrinalpha5 and delta/notch signaling have complementary spatiotemporal requirements during zebrafish somitogenesis. *Dev. Cell* **8**, 575-586.

Karlstrom, R. O., Talbot, W. S. and Schier, A. F. (1999). Comparative synteny cloning of zebrafish you-too: mutations in the Hedgehog target gli2 affect ventral forebrain patterning. *Genes Dev.* **13**, 388-393.

Kawakami, A., Nojima, Y., Toyoda, A., Takahoko, M., Satoh, M., Tanaka, H., Wada, H., Masai, I., Terasaki, H., Sakaki, Y. et al. (2005). The zebrafish-secreted matrix protein you/scube2 is implicated in long-range regulation of hedgehog signaling. *Curr. Biol.* **15**, 480-488.

Kelsh, R. N. (2004). Genetics and evolution of pigment patterns in fish. *Pigment Cell Res.* **17**, 326-336.

Kelsh, R. N. and Eisen, J. S. (2000). The zebrafish *colourless* gene regulates development of non-ectomesenchymal neural crest derivatives. *Development* **127**, 515-525.

Kelsh, R. N., Brand, M., Jiang, Y. J., Heisenberg, C. P., Lin, S., Haffter, P., Odenthal, J., Mullins, M. C., van Eeden, F. J., Furutani-Seiki, M. et al. (1996). Zebrafish pigmentation mutations and the processes of neural crest development. *Development* **123**, 369-389.

Kelsh, R. N., Dutton, K., Medlin, J. and Eisen, J. S. (2000a). Expression of zebrafish *fkd6* in neural crest-derived glia. *Mech. Dev.* **93**, 161-164.

Kelsh, R. N., Schmid, B. and Eisen, J. S. (2000b). Genetic analysis of melanophore development in Zebrafish embryos. *Dev. Biol.* **225**, 277-293.

Kimmel, C. B. and Warga, R. M. (1987). Indeterminate cell lineage of the Zebrafish embryo. *Dev. Biol.* **124**, 269-280.

Kimmel, C. B., Ballard, W. W., Kimmel, S. R., Ullmann, B. and Schilling, T. F. (1995). Stages of embryonic development of the Zebrafish. *Dev. Dyn.* **203**, 253-310.

Knaut, H., Werz, C., Geisler, R. and Nusslein-Volhard, C. (2003). A zebrafish homologue of the chemokine receptor Cxcr4 is a germ-cell guidance receptor. *Nature* **421**, 279-282.
Krull, C. E. (2001). Segmental organization of neural crest migration. *Mech. Dev.* **105**, 37-45.
Lallier, T. E. and Bronner-Fraser, M. (1988). A spatial and temporal analysis of dorsal root and sympathetic ganglion formation in the avian embryo. *Dev. Biol.* **127**, 99-112.
Lewis, K. E., Currie, P. D., Roy, S., Schauerte, H., Haffter, P. and Ingham, P. W. (1999). Control of muscle cell-type specification in the zebrafish embryo by Hedgehog signalling. *Dev. Biol.* **216**, 469-480.
Li, Q., Shirabe, K. and Kuwada, J. Y. (2004). Chemokine signaling regulates sensory cell migration in zebrafish. *Dev. Biol.* **269**, 123-136.
Li, Q., Shirabe, K., Thisse, C., Thisse, B., Okamoto, H., Masai, I. and Kuwada, J. Y. (2005). Chemokine signaling guides axons within the retina in zebrafish. *J. Neurosci.* **25**, 1711-1717.
Li, Y. X., Zdanowicz, M., Young, L., Kumiski, D., Leatherbury, L. and Kirby, M. L. (2003). Cardiac neural crest in zebrafish embryos contributes to myocardial cell lineage and early heart function. *Dev. Dyn.* **226**, 540-550.
Lister, J. A., Robertson, C. P., Lepage, T., Johnson, S. L. and Raible, D. W. (1999). nacre encodes a zebrafish microphthalmia-related protein that regulates neural-crest-derived pigment cell fate. *Development* **126**, 3757-3767.
Loetscher, M., Geiser, T., O'Reilly, T., Zwahlen, R., Baggiolini, M. and Moser, B. (1994). Cloning of a human seven-transmembrane domain receptor, LESTR, that is highly expressed in leukocytes. *J. Biol. Chem.* **269**, 232-237.
Löfberg, J., Nynas-McCoy, A., Olsson, C., Jonsson, L. and Perris, R. (1985). Stimulation of initial neural crest cell migration in the axolotl embryo by tissue grafts and extracellular matrix transplanted on microcarriers. *Dev. Biol.* **107**, 442-459.
Löfberg, J., Perris, R. and Epperlein, H. H. (1989). Timing in the regulation of neural crest cell migration: retarded "maturation" of regional extracellular matrix inhibits pigment cell migration in embryos of the white axolotl mutant. *Dev. Biol.* **131**, 168-181.
Lyon, M. F. and Searle, A. G. (1989). *Genetic Variants and Strains of the Laboratory Mouse*. Oxford: Oxford University Press.
Marusich, M. F., Furneaux, H. M., Henion, P. D. and Weston, J. A. (1994). Hu neuronal proteins are expressed in proliferating neurogenic cells. *J. Neurobiol.* **25**, 143-155.
Nakano, Y., Kim, H. R., Kawakami, A., Roy, S., Schier, A. F. and Ingham, P. W. (2004). Inactivation of dispatched 1 by the chameleon mutation disrupts Hedgehog signalling in the zebrafish embryo. *Dev. Biol.* **269**, 381-392.
Neyt, C., Jagla, K., Thisse, C., Thisse, B., Haines, L. and Currie, P. D. (2000). Evolutionary origins of vertebrate appendicular muscle. *Nature* **408**, 82-86.
Oberlin, E., Amara, A., Bachelerie, F., Bessia, C., Virelizier, J. L., Arenzana-Seisdedos, F., Schwartz, O., Heard, J. M., Clark-Lewis, I., Legler, D. F. et al. (1996). The CXC chemokine SDF-1 is the ligand for LESTR/fusin and prevents infection by T-cell-line-adapted HIV-1. *Nature* **382**, 833-835.
Odenthal, J., Rossnagel, K., Haffter, P., Kelsh, R., Vogelsang, E., Brand, M., van Eeden, F., Furutani-Seiki, M., Granato, M., Hammerschmidt, M. et al. (1996). Mutations affecting xanthophore pigmentation in the zebrafish, Danio rerio. *Development* **123**, 391-398.
Parichy, D. M. and Turner, J. M. (2003). Temporal and cellular requirements for Fms signaling during zebrafish adult pigment pattern development. *Development* **130**, 817-833.
Parichy, D. M., Mellgren, E. M., Rawls, J. F., Lopes, S. S., Kelsh, R. N. and Johnson, S. L. (2000a). Mutational analysis of endothelin receptor b1 (rose) during neural crest and pigment pattern development in the zebrafish danio rerio. *Dev. Biol.* **227**, 294-306.
Parichy, D. M., Ransom, D. G., Paw, B., Zon, L. I. and Johnson, S. L. (2000b). An orthologue of the kit-related gene fms is required for development of neural crest-derived xanthophores and a subpopulation of adult melanocytes in the zebrafish, Danio rerio. *Development* **127**, 3031-3044.
Perris, R. and Perissinotto, D. (2000). Role of the extracellular matrix during neural crest cell migration. *Mech. Dev.* **95**, 3-21.
Quigley, I. K., Turner, J. M., Nuckels, R. J., Manuel, J. L., Budi, E. H., MacDonald, E. L. and Parichy, D. M. (2004). Pigment pattern evolution by differential deployment of neural crest and post-embryonic melanophore lineages in Danio fishes. *Development* **131**, 6053-6069.
Rawls, J. F. and Johnson, S. L. (2001). Requirements for the kit receptor tyrosine kinase during regeneration of zebrafish fin melanocytes. *Development* **128**, 1943-1949.
Rickmann, M., Fawcett, J. W. and Keynes, R. J. (1985). The migration of neural crest cells and the growth of motor axons through the rostral half of the chick somite. *J. Embryol. Exp. Morphol.* **90**, 437-455.
Santiago, A. and Erickson, C. A. (2002). Ephrin-B ligands play a dual role in the control of neural crest cell migration. *Development* **129**, 3621-3632.
Sato, M. and Yost, H. J. (2003). Cardiac neural crest contributes to cardiomyogenesis in zebrafish. *Dev. Biol.* **257**, 127-139.
Schauerte, H. E., van Eeden, F. J., Fricke, C., Odenthal, J., Strahle, U. and Haffter, P. (1998). Sonic hedgehog is not required for the induction of medial floor plate cells in the zebrafish. *Development* **125**, 2983-2993.
Schier, A. F. (2003). Chemokine signaling: rules of attraction. *Curr. Biol.* **13**, R192-R194.
Schilling, T. F. and Kimmel, C. B. (1994). Segment and cell type lineage restrictions during pharyngeal arch development in the zebrafish embryo. *Development* **120**, 483-494.
van Eeden, F., Granato, M., Schach, U., Brand, M., Furutani-Seiki, M., Haffter, P., Hammerschmidt, M., Heisenberg, C., Jiang, Y., Kane, D. et al. (1996). Mutations affecting somite formation and patterning in the zebrafish, Danio rerio. *Development* **123**, 153-164.
Waterman, R. E. (1969). Development of the lateral musculature in the teleost, *Brachydanio rerio*: a fine structural study. *Am. J. Anat.* **125**, 457-493.
Wehrle-Haller, B. and Weston, J. A. (1995). Soluble and cell-bound forms of steel factor activity play distinct roles in melanocyte precursor dispersal and survival on the lateral neural crest migration pathway. *Development* **121**, 731-742.
Woods, I. G. and Talbot, W. S. (2005). The you gene encodes an EGF-CUB protein essential for Hedgehog signaling in zebrafish. *PLoS Biol.* **3**, e66.